PHYSICAL REVIEW D **89,** 111103(R) (2014)

Study of the reaction $e^+e^- \to \psi(2S)\pi^+\pi^-$ via initial-state radiation at *BABAR*

J. P. Lees,[1] V. Poireau,[1] V. Tisserand,[1] J. Garra Tico,[2] E. Grauges,[2] A. Palano,[3a,3b] G. Eigen,[4] B. Stugu,[4] D. N. Brown,[5] L. T. Kerth,[5] Yu. G. Kolomensky,[5] G. Lynch,[5] H. Koch,[6] T. Schroeder,[6] D. J. Asgeirsson,[7] C. Hearty,[7] T. S. Mattison,[7] J. A. McKenna,[7] R. Y. So,[7] A. Khan,[8] V. E. Blinov,[9] A. R. Buzykaev,[9] V. P. Druzhinin,[9] V. B. Golubev,[9] E. A. Kravchenko,[9] A. P. Onuchin,[9] S. I. Serednyakov,[9] Yu. I. Skovpen,[9] E. P. Solodov,[9] K. Yu. Todyshev,[9] A. N. Yushkov,[9] M. Bondioli,[10] D. Kirkby,[10] A. J. Lankford,[10] M. Mandelkern,[10] H. Atmacan,[11] J. W. Gary,[11] F. Liu,[11] O. Long,[11] G. M. Vitug,[11] C. Campagnari,[12] T. M. Hong,[12] D. Kovalskyi,[12] J. D. Richman,[12] C. A. West,[12] A. M. Eisner,[13] J. Kroseberg,[13] W. S. Lockman,[13] A. J. Martinez,[13] B. A. Schumm,[13] A. Seiden,[13] D. S. Chao,[14] C. H. Cheng,[14] B. Echenard,[14] K. T. Flood,[14] D. G. Hitlin,[14] P. Ongmongkolkul,[14] F. C. Porter,[14] A. Y. Rakitin,[14] R. Andreassen,[15] Z. Huard,[15] B. T. Meadows,[15] M. D. Sokoloff,[15] L. Sun,[15] P. C. Bloom,[16] W. T. Ford,[16] A. Gaz,[16] U. Nauenberg,[16] J. G. Smith,[16] S. R. Wagner,[16] R. Ayad,[17,¶] W. H. Toki,[17] B. Spaan,[18] K. R. Schubert,[19] R. Schwierz,[19] D. Bernard,[20] M. Verderi,[20] P. J. Clark,[21] S. Playfer,[21] D. Bettoni,[22a] C. Bozzi,[22a] R. Calabrese,[22a,22b] G. Cibinetto,[22a,22b] E. Fioravanti,[22a,22b] I. Garzia,[22a,22b] E. Luppi,[22a,22b] M. Munerato,[22a,22b] M. Negrini,[22a,22b] L. Piemontese,[22a] V. Santoro,[22a] R. Baldini-Ferroli,[23] A. Calcaterra,[23] R. de Sangro,[23] G. Finocchiaro,[23] P. Patteri,[23] I. M. Peruzzi,[23,†] M. Piccolo,[23] M. Rama,[23] A. Zallo,[23] R. Contri,[24a,24b] E. Guido,[24a,24b] M. Lo Vetere,[24a,24b] M. R. Monge,[24a,24b] S. Passaggio,[24a] C. Patrignani,[24a,24b] E. Robutti,[24a] B. Bhuyan,[25] V. Prasad,[25] C. L. Lee,[26] M. Morii,[26] A. J. Edwards,[27] A. Adametz,[28] U. Uwer,[28] H. M. Lacker,[29] T. Lueck,[29] P. D. Dauncey,[30] P. K. Behera,[31] U. Mallik,[31] C. Chen,[32] J. Cochran,[32] W. T. Meyer,[32] S. Prell,[32] A. E. Rubin,[32] A. V. Gritsan,[33] Z. J. Guo,[33] N. Arnaud,[34] M. Davier,[34] D. Derkach,[34] G. Grosdidier,[34] F. Le Diberder,[34] A. M. Lutz,[34] B. Malaescu,[34] P. Roudeau,[34] M. H. Schune,[34] A. Stocchi,[34] G. Wormser,[34] D. J. Lange,[35] D. M. Wright,[35] C. A. Chavez,[36] J. P. Coleman,[36] J. R. Fry,[36] E. Gabathuler,[36] D. E. Hutchcroft,[36] D. J. Payne,[36] C. Touramanis,[36] A. J. Bevan,[37] F. Di Lodovico,[37] R. Sacco,[37] M. Sigamani,[37] G. Cowan,[38] D. N. Brown,[39] C. L. Davis,[39] A. G. Denig,[40] M. Fritsch,[40] W. Gradl,[40] K. Griessinger,[40] A. Hafner,[40] E. Prencipe,[40] R. J. Barlow,[41,‡] G. Jackson,[41] G. D. Lafferty,[41] E. Behn,[42] R. Cenci,[42] B. Hamilton,[42] A. Jawahery,[42] D. A. Roberts,[42] C. Dallapiccola,[43] R. Cowan,[44] D. Dujmic,[44] G. Sciolla,[44] R. Cheaib,[45] D. Lindemann,[45] P. M. Patel,[45] S. H. Robertson,[45] P. Biassoni,[46a,46b] N. Neri,[46a] F. Palombo,[46a,46b] S. Stracka,[46a,46b] L. Cremaldi,[47] R. Godang,[47,§] R. Kroeger,[47] P. Sonnek,[47] D. J. Summers,[47] X. Nguyen,[48] M. Simard,[48] P. Taras,[48] G. De Nardo,[49a,49b] D. Monorchio,[49a,49b] G. Onorato,[49a,49b] C. Sciacca,[49a,49b] M. Martinelli,[50] G. Raven,[50] C. P. Jessop,[51] J. M. LoSecco,[51] W. F. Wang,[51] K. Honscheid,[52] R. Kass,[52] J. Brau,[53] R. Frey,[53] N. B. Sinev,[53] D. Strom,[53] E. Torrence,[53] E. Feltresi,[54a,54b] N. Gagliardi,[54a,54b] M. Margoni,[54a,54b] M. Morandin,[54a] M. Posocco,[54a] M. Rotondo,[54a] G. Simi,[54a] F. Simonetto,[54a,54b] R. Stroili,[54a,54b] S. Akar,[55] E. Ben-Haim,[55] M. Bomben,[55] G. R. Bonneaud,[55] H. Briand,[55] G. Calderini,[55] J. Chauveau,[55] O. Hamon,[55] Ph. Leruste,[55] G. Marchiori,[55] J. Ocariz,[55] S. Sitt,[55] M. Biasini,[56a,56b] E. Manoni,[56a,56b] S. Pacetti,[56a,56b] A. Rossi,[56a,56b] C. Angelini,[57a,57b] G. Batignani,[57a,57b] S. Bettarini,[57a,57b] M. Carpinelli,[57a,57b,‖] G. Casarosa,[57a,57b] A. Cervelli,[57a,57b] F. Forti,[57a,57b] M. A. Giorgi,[57a,57b] A. Lusiani,[57a,57c] B. Oberhof,[57a,57b] E. Paoloni,[57a,57b] A. Perez,[57a] G. Rizzo,[57a,57b] J. J. Walsh,[57a] D. Lopes Pegna,[58] J. Olsen,[58] A. J. S. Smith,[58] A. V. Telnov,[58] F. Anulli,[59a] R. Faccini,[59a,59b] F. Ferrarotto,[59a] F. Ferroni,[59a,59b] M. Gaspero,[59a,59b] L. Li Gioi,[59a] M. A. Mazzoni,[59a] G. Piredda,[59a] C. Bünger,[60] O. Grünberg,[60] T. Hartmann,[60] T. Leddig,[60] H. Schröder,[60,*] C. Voß,[60] R. Waldi,[60] T. Adye,[61] E. O. Olaiya,[61] F. F. Wilson,[61] S. Emery,[62] G. Hamel de Monchenault,[62] G. Vasseur,[62] Ch. Yèche,[62] D. Aston,[63] D. J. Bard,[63] R. Bartoldus,[63] J. F. Benitez,[63] C. Cartaro,[63] M. R. Convery,[63] J. Dorfan,[63] G. P. Dubois-Felsmann,[63] W. Dunwoodie,[63] M. Ebert,[63] R. C. Field,[63] M. Franco Sevilla,[63] B. G. Fulsom,[63] A. M. Gabareen,[63] M. T. Graham,[63] P. Grenier,[63] C. Hast,[63] W. R. Innes,[63] M. H. Kelsey,[63] P. Kim,[63] M. L. Kocian,[63] D. W. G. S. Leith,[63] P. Lewis,[63] B. Lindquist,[63] S. Luitz,[63] V. Luth,[63] H. L. Lynch,[63] D. B. MacFarlane,[63] D. R. Muller,[63] H. Neal,[63] S. Nelson,[63] M. Perl,[63] T. Pulliam,[63] B. N. Ratcliff,[63] A. Roodman,[63] A. A. Salnikov,[63] R. H. Schindler,[63] A. Snyder,[63] D. Su,[63] M. K. Sullivan,[63] J. Va'vra,[63] A. P. Wagner,[63] W. J. Wisniewski,[63] M. Wittgen,[63] D. H. Wright,[63] H. W. Wulsin,[63] C. C. Young,[63] V. Ziegler,[63] W. Park,[64] M. V. Purohit,[64] R. M. White,[64] J. R. Wilson,[64] A. Randle-Conde,[65] S. J. Sekula,[65] M. Bellis,[66] P. R. Burchat,[66] T. S. Miyashita,[66] M. S. Alam,[67] J. A. Ernst,[67] R. Gorodeisky,[68] N. Guttman,[68] D. R. Peimer,[68] A. Soffer,[68] P. Lund,[69] S. M. Spanier,[69] J. L. Ritchie,[70] A. M. Ruland,[70] R. F. Schwitters,[70] B. C. Wray,[70] J. M. Izen,[71] X. C. Lou,[71] F. Bianchi,[72a,72b] D. Gamba,[72a,72b] S. Zambito,[72a,72b] L. Lanceri,[73a,73b] L. Vitale,[73a,73b] F. Martinez-Vidal,[74] A. Oyanguren,[74] H. Ahmed,[75] J. Albert,[75] Sw. Banerjee,[75] F. U. Bernlochner,[75] H. H. F. Choi,[75] G. J. King,[75] R. Kowalewski,[75] M. J. Lewczuk,[75] I. M. Nugent,[75] J. M. Roney,[75] R. J. Sobie,[75] N. Tasneem,[75] T. J. Gershon,[76] P. F. Harrison,[76] T. E. Latham,[76] E. M. T. Puccio,[76] H. R. Band,[77] S. Dasu,[77] Y. Pan,[77] R. Prepost,[77] and S. L. Wu[77]

(*BABAR* Collaboration)

[1]*Laboratoire d'Annecy-le-Vieux de Physique des Particules (LAPP), Université de Savoie, CNRS/IN2P3, F-74941 Annecy-Le-Vieux, France*

[2]*Universitat de Barcelona, Facultat de Fisica, Departament ECM, E-08028 Barcelona, Spain*
[3a]*INFN Sezione di Bari, I-70126 Bari, Italy*
[3b]*Dipartimento di Fisica, Università di Bari, I-70126 Bari, Italy*
[4]*University of Bergen, Institute of Physics, N-5007 Bergen, Norway*
[5]*Lawrence Berkeley National Laboratory and University of California, Berkeley, California 94720, USA*
[6]*Ruhr Universität Bochum, Institut für Experimentalphysik 1, D-44780 Bochum, Germany*
[7]*University of British Columbia, Vancouver, British Columbia, Canada V6T 1Z1*
[8]*Brunel University, Uxbridge, Middlesex UB8 3PH, United Kingdom*
[9]*Budker Institute of Nuclear Physics, Novosibirsk 630090, Russia*
[10]*University of California at Irvine, Irvine, California 92697, USA*
[11]*University of California at Riverside, Riverside, California 92521, USA*
[12]*University of California at Santa Barbara, Santa Barbara, California 93106, USA*
[13]*University of California at Santa Cruz, Institute for Particle Physics, Santa Cruz, California 95064, USA*
[14]*California Institute of Technology, Pasadena, California 91125, USA*
[15]*University of Cincinnati, Cincinnati, Ohio 45221, USA*
[16]*University of Colorado, Boulder, Colorado 80309, USA*
[17]*Colorado State University, Fort Collins, Colorado 80523, USA*
[18]*Technische Universität Dortmund, Fakultät Physik, D-44221 Dortmund, Germany*
[19]*Technische Universität Dresden, Institut für Kern- und Teilchenphysik, D-01062 Dresden, Germany*
[20]*Laboratoire Leprince-Ringuet, Ecole Polytechnique, CNRS/IN2P3, F-91128 Palaiseau, France*
[21]*University of Edinburgh, Edinburgh EH9 3JZ, United Kingdom*
[22a]*INFN Sezione di Ferrara, I-44100 Ferrara, Italy*
[22b]*Dipartimento di Fisica, Università di Ferrara, I-44100 Ferrara, Italy*
[23]*INFN Laboratori Nazionali di Frascati, I-00044 Frascati, Italy*
[24a]*INFN Sezione di Genova, I-16146 Genova, Italy*
[24b]*Dipartimento di Fisica, Università di Genova, I-16146 Genova, Italy*
[25]*Indian Institute of Technology Guwahati, Guwahati, Assam, 781 039, India*
[26]*Harvard University, Cambridge, Massachusetts 02138, USA*
[27]*Harvey Mudd College, Claremont, California 91711*
[28]*Universität Heidelberg, Physikalisches Institut, Philosophenweg 12, D-69120 Heidelberg, Germany*
[29]*Humboldt-Universität zu Berlin, Institut für Physik, Newtonstrasse 15, D-12489 Berlin, Germany*
[30]*Imperial College London, London, SW7 2AZ, United Kingdom*
[31]*University of Iowa, Iowa City, Iowa 52242, USA*
[32]*Iowa State University, Ames, Iowa 50011-3160, USA*
[33]*Johns Hopkins University, Baltimore, Maryland 21218, USA*
[34]*Laboratoire de l'Accélérateur Linéaire, IN2P3/CNRS et Université Paris-Sud 11, Centre Scientifique d'Orsay, B. P. 34, F-91898 Orsay Cedex, France*
[35]*Lawrence Livermore National Laboratory, Livermore, California 94550, USA*
[36]*University of Liverpool, Liverpool L69 7ZE, United Kingdom*
[37]*Queen Mary, University of London, London, E1 4NS, United Kingdom*
[38]*University of London, Royal Holloway and Bedford New College, Egham, Surrey TW20 0EX, United Kingdom*
[39]*University of Louisville, Louisville, Kentucky 40292, USA*
[40]*Johannes Gutenberg-Universität Mainz, Institut für Kernphysik, D-55099 Mainz, Germany*
[41]*University of Manchester, Manchester M13 9PL, United Kingdom*
[42]*University of Maryland, College Park, Maryland 20742, USA*
[43]*University of Massachusetts, Amherst, Massachusetts 01003, USA*
[44]*Massachusetts Institute of Technology, Laboratory for Nuclear Science, Cambridge, Massachusetts 02139, USA*
[45]*McGill University, Montréal, Québec, Canada H3A 2T8*
[46a]*INFN Sezione di Milano, I-20133 Milano, Italy*
[46b]*Dipartimento di Fisica, Università di Milano, I-20133 Milano, Italy*
[47]*University of Mississippi, University, Mississippi 38677, USA*
[48]*Université de Montréal, Physique des Particules, Montréal, Québec, Canada H3C 3J7*
[49a]*INFN Sezione di Napoli, I-80126 Napoli, Italy*
[49b]*Dipartimento di Scienze Fisiche, Università di Napoli Federico II, I-80126 Napoli, Italy*
[50]*NIKHEF, National Institute for Nuclear Physics and High Energy Physics, NL-1009 DB Amsterdam, The Netherlands*
[51]*University of Notre Dame, Notre Dame, Indiana 46556, USA*
[52]*Ohio State University, Columbus, Ohio 43210, USA*

[53]University of Oregon, Eugene, Oregon 97403, USA
[54a]INFN Sezione di Padova, I-35131 Padova, Italy
[54b]Dipartimento di Fisica, Università di Padova, I-35131 Padova, Italy
[55]Laboratoire de Physique Nucléaire et de Hautes Energies, IN2P3/CNRS, Université Pierre et Marie Curie-Paris6, Université Denis Diderot-Paris7, F-75252 Paris, France
[56a]INFN Sezione di Perugia, I-06100 Perugia, Italy
[56b]Dipartimento di Fisica, Università di Perugia, I-06100 Perugia, Italy
[57a]INFN Sezione di Pisa, I-56127 Pisa, Italy
[57b]Dipartimento di Fisica, Università di Pisa, I-56127 Pisa, Italy
[57c]Scuola Normale Superiore di Pisa, I-56127 Pisa, Italy
[58]Princeton University, Princeton, New Jersey 08544, USA
[59a]INFN Sezione di Roma, I-00185 Roma, Italy
[59b]Dipartimento di Fisica, Università di Roma La Sapienza, I-00185 Roma, Italy
[60]Universität Rostock, D-18051 Rostock, Germany
[61]Rutherford Appleton Laboratory, Chilton, Didcot, Oxon, OX11 0QX, United Kingdom
[62]CEA, Irfu, SPP, Centre de Saclay, F-91191 Gif-sur-Yvette, France
[63]SLAC National Accelerator Laboratory, Stanford, California 94309 USA
[64]University of South Carolina, Columbia, South Carolina 29208, USA
[65]Southern Methodist University, Dallas, Texas 75275, USA
[66]Stanford University, Stanford, California 94305-4060, USA
[67]State University of New York, Albany, New York 12222, USA
[68]Tel Aviv University, School of Physics and Astronomy, Tel Aviv, 69978, Israel
[69]University of Tennessee, Knoxville, Tennessee 37996, USA
[70]University of Texas at Austin, Austin, Texas 78712, USA
[71]University of Texas at Dallas, Richardson, Texas 75083, USA
[72a]INFN Sezione di Torino, I-10125 Torino, Italy
[72b]Dipartimento di Fisica Sperimentale, Università di Torino, I-10125 Torino, Italy
[73a]INFN Sezione di Trieste, I-34127 Trieste, Italy
[73b]Dipartimento di Fisica, Università di Trieste, I-34127 Trieste, Italy
[74]IFIC, Universitat de Valencia-CSIC, E-46071 Valencia, Spain
[75]University of Victoria, Victoria, British Columbia, Canada V8W 3P6
[76]Department of Physics, University of Warwick, Coventry CV4 7AL, United Kingdom
[77]University of Wisconsin, Madison, Wisconsin 53706, USA

(Received 29 November 2012; published 25 June 2014)

We study the process $e^+e^- \to \psi(2S)\pi^+\pi^-$ with initial-state-radiation events produced at the PEP-II asymmetric-energy collider. The data were recorded with the *BABAR* detector at center-of-mass energies at and near the $\Upsilon(\mathrm{nS})$ $(n = 2, 3, 4)$ resonances and correspond to an integrated luminosity of 520 fb^{-1}. We investigate the $\psi(2S)\pi^+\pi^-$ mass distribution from 3.95 to 5.95 GeV/c^2, and measure the center-of-mass energy dependence of the associated $e^+e^- \to \psi(2S)\pi^+\pi^-$ cross section. The mass distribution exhibits evidence of two resonant structures. A fit to the $\psi(2S)\pi^+\pi^-$ mass distribution corresponding to the decay mode $\psi(2S) \to J/\psi\pi^+\pi^-$ yields a mass value of $4340 \pm 16\,(\mathrm{stat}) \pm 9\,(\mathrm{syst})$ MeV/c^2 and a width of $94 \pm 32\,(\mathrm{stat}) \pm 13\,(\mathrm{syst})$ MeV for the first resonance, and for the second a mass value of $4669 \pm 21\,(\mathrm{stat}) \pm 3\,(\mathrm{syst})$ MeV/c^2 and a width of $104 \pm 48\,(\mathrm{stat}) \pm 10\,(\mathrm{syst})$ MeV. In addition, we show the $\pi^+\pi^-$ mass distributions for these resonant regions.

DOI: 10.1103/PhysRevD.89.111103 PACS numbers: 13.20.Gd, 13.25.Gv, 13.66.Bc, 14.40.Pq

Many new $c\bar{c}$ or charmoniumlike states have been discovered at the B factories in the energy region above the $D\bar{D}$ threshold. Of these, the $X(3872)$ [1], $\chi_{c2}(2P)(3930)$ [2], $Y(3940)$ [3], and $Y(4260)$ [4] resonances are now well established. Since the $Y(4260)$ is produced via initial-state radiation (ISR) in the reaction $e^+e^- \to \gamma_{\mathrm{ISR}}J/\psi\pi^+\pi^-$, it has $J^{PC} = 1^{--}$. In addition to the $Y(4260)$, two more $J^{PC} = 1^{--}$ states, the $Y(4360)$ and the $Y(4660)$, have been reported in ISR production, via $e^+e^- \to \gamma_{\mathrm{ISR}}\psi(2S)\pi^+\pi^-$ [5,6]. The $Y(4660)$ has been observed only in the Belle experiment [6], and so it is important to confirm the existence of this state.

[*]Deceased.
[†]Also at Università di Perugia, Dipartimento di Fisica, Perugia, Italy.
[‡]Present address: the University of Huddersfield, Huddersfield HD1 3DH, UK.
[§]Present address: University of South Alabama, Mobile, Alabama 36688, USA.
[‖]Also at Università di Sassari, Sassari, Italy.
[¶]Present address: the University of Tabuk, Tabuk 71491, Saudi Arabia.

In this paper we utilize the ISR mechanism to study the reaction $e^+e^- \to \psi(2S)\pi^+\pi^-$ in the center-of-mass (c.m.) energy (E_{cm}) range 3.95–5.95 GeV, where the $\psi(2S)$ decays to $J/\psi\pi^+\pi^-$ or to l^+l^-, with l^+l^- representing either e^+e^- or $\mu^+\mu^-$.

We use a data sample corresponding to an integrated luminosity of 520 fb^{-1} [7], recorded with the *BABAR* detector at the SLAC PEP-II asymmetric-energy e^+e^- collider operating at and near the c.m. energies of the $\Upsilon(\text{nS})$ $(n = 2, 3, 4)$ resonances. The detector is described in detail elsewhere [8]. Charged-particle momenta are measured in a tracking system consisting of a five-layer, double-sided, silicon vertex-tracker (SVT) and a 40-layer central drift chamber (DCH), both coaxial with the 1.5 T magnetic field of a superconducting solenoid. An internally reflecting ring-imaging Cherenkov detector and specific ionization measurements from the SVT and DCH provide charged-particle identification (PID). A CsI(Tl) electromagnetic calorimeter (EMC) detects and identifies photons and electrons. Muons are identified using information from the instrumented flux-return system.

We reconstruct events corresponding to the reaction $e^+e^- \to \gamma_{\text{ISR}}\psi(2S)\pi^+\pi^-$, where γ_{ISR} represents a photon that is radiated from the initial-state e^+ or e^-, thus lowering the c.m. energy of the e^+e^- collision that produces the $\psi(2S)\pi^+\pi^-$ system. We do not require observation of the ISR photon, since it would be detectable in the EMC for only ∼15% of the events.

For the $\psi(2S) \to J/\psi\pi^+\pi^-$ decay mode, we select events containing exactly six charged-particle tracks, and reconstruct J/ψ candidates via their decay to e^+e^- or $\mu^+\mu^-$. For each mode, at least one of the leptons must be identified on the basis of PID information. When possible, electron candidates are combined with photons to recover bremsstrahlung energy loss in order to improve the J/ψ momentum measurement. An e^+e^- pair with invariant mass within $(-60, +45)$ MeV/c^2 of the nominal J/ψ mass [9] is accepted as a J/ψ candidate, as is a $\mu^+\mu^-$ pair with mass within $(-45, +45)$ MeV/c^2 of this value. Each J/ψ candidate is subjected to a geometric fit in which the decay vertex is constrained to the e^+e^- collision axis within the interaction region; the χ^2 probability of the fit must be greater than 0.001. An accepted J/ψ candidate is kinematically constrained to the nominal J/ψ mass [9] and combined with a pion pair to form a $\psi(2S) \to J/\psi\pi^+\pi^-$ candidate. The pions must be identified using PID information. The $J/\psi\pi^+\pi^-$ combinations with invariant mass within 10 MeV/c^2 of the nominal $\psi(2S)$ mass [9] are considered to be within the $\psi(2S)$ signal region and are taken as $\psi(2S)$ candidates. The $\psi(2S)$ candidate is refit requiring that the χ^2 probability for the vertex fit be greater than 0.001. A further geometric fit with the $\psi(2S)$ candidate mass constrained to the nominal mass value is performed. A surviving candidate is then combined with two additional pions of opposite charge, each of which is identified using PID information, to reconstruct a $\psi(2S)\pi^+\pi^-$ candidate.

For the decay mode $\psi(2S) \to l^+l^-$, we select events containing exactly four charged-particle tracks and reconstruct $\psi(2S)$ candidates via their decay to e^+e^- or $\mu^+\mu^-$. An e^+e^- $[\mu^+\mu^-]$ pair with invariant mass within $(-40, +30)$ MeV/c^2 $[(-30, +30)$ MeV/$c^2]$ of the nominal $\psi(2S)$ mass is accepted as being within the $\psi(2S)$ signal region. Each such candidate is subjected to the same geometrical fit and mass constraint procedure as applied for the $\psi(2S) \to J/\psi\pi^+\pi^-$ mode. A surviving candidate is combined with a pion pair to form a $\psi(2S)\pi^+\pi^-$ candidate.

For $\psi(2S) \to J/\psi\pi^+\pi^-$ $[\psi(2S) \to l^+l^-]$, the difference between the c.m. momentum of the hadronic $\psi(2S)\pi^+\pi^-$ system and the value expected for an ISR event [i.e. $(s - m^2)/2\sqrt{s}$, where m is the $\psi(2S)\pi^+\pi^-$ invariant mass] must be in the range $(-0.10, +0.70)$ GeV/c $[(-0.70, +0.60)$ GeV/$c]$ to be consistent with an ISR photon. We require the transverse component of the missing momentum to be less than 2.0 GeV/c [1.7 GeV/c]. If the ISR photon is detected in the EMC, its momentum vector is added to that of the $\psi(2S)\pi^+\pi^-$ system in calculating the missing momentum. For $\psi(2S) \to e^+e^-$ events, the candidate $\pi^+\pi^-$ system has a small contamination due to e^+e^- pairs from photon conversions. We compute the pair invariant mass $m_{e^+e^-}$, with the electron mass assigned to each pion candidate and remove candidates with $m_{e^+e^-} < 100$ MeV/c^2.

For events with multiple $\psi(2S)$ candidates, we select the combination that has candidate mass closest to the nominal $\psi(2S)$ mass [9]. We estimate the remaining background for the $\psi(2S) \to J/\psi\pi^+\pi^-$ candidates using the sideband regions (3.566, 3.666) and (3.706, 3.806) GeV/c^2 in the $J/\psi\pi^+\pi^-$ invariant mass distribution. The sideband events are identified before the geometric fit with the constraint to the $\psi(2S)$ mass is applied. For $\psi(2S) \to e^+e^-$, the corresponding sideband regions are (3.476, 3.576) and (3.776, 3.876) GeV/c^2, while for $\psi(2S) \to \mu^+\mu^-$ the sideband regions are (3.516, 3.596) and (3.776, 3.856) GeV/c^2.

Figure 1 shows the $\psi(2S)\pi^+\pi^-$ invariant mass distributions for the selected $\psi(2S)$ events corresponding to the decays (a) $\psi(2S) \to J/\psi\pi^+\pi^-$, (b) $\psi(2S) \to l^+l^-$, and (c) the combined sample for $\psi(2S) \to J/\psi\pi^+\pi^-$ and $\psi(2S) \to l^+l^-$. The background is estimated from the $\psi(2S)$ mass sidebands as described above. In Fig. 1 two structures are evident, the first near 4.35 GeV/c^2 and the second near 4.65 GeV/c^2. We attribute these peaks to the $Y(4360)$ [5] and to the $Y(4660)$ [6], respectively. We perform an unbinned, extended, maximum-likelihood (ML) fit to the results shown in Fig. 1(a) in order to extract the parameter values of the resonances. The background is described by fitting a fourth-order polynomial to the background distribution determined from the sidebands [note that the

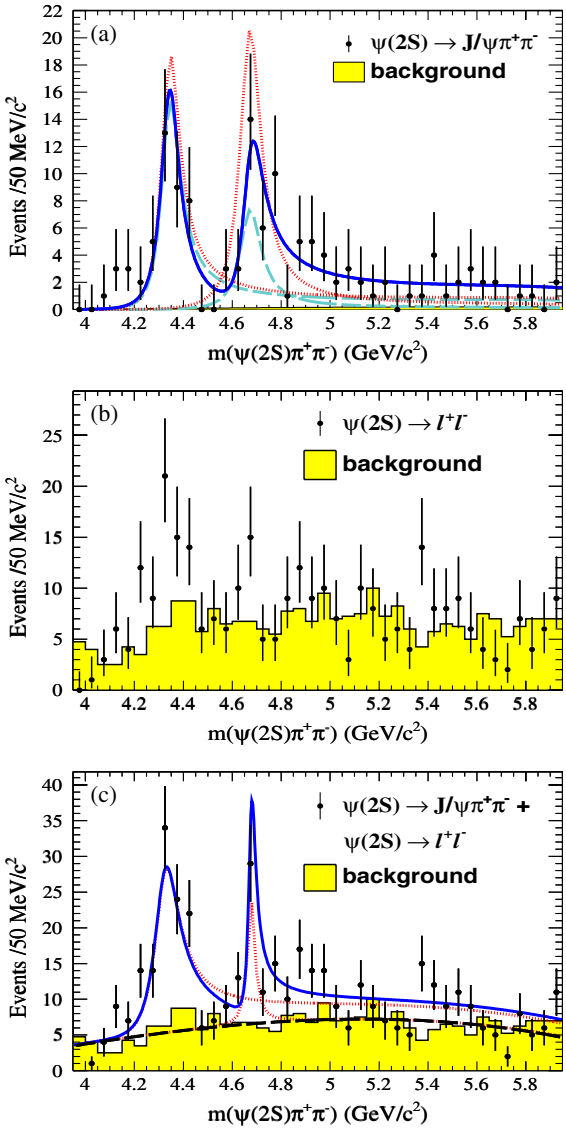

FIG. 1 (color online). (a) The $\psi(2S)\pi^+\pi^-$ invariant mass distribution from the kinematic threshold to 5.95 GeV/c^2 for $\psi(2S) \to J/\psi\pi^+\pi^-$; the points with error bars represent the data in the $\psi(2S)$ signal region, and the shaded histogram is the background estimated from the $\psi(2S)$ sideband regions. The solid curve shows the result of the fit described in the text. The dashed (dotted) curves indicate the individual resonant contributions for constructive (destructive) interference. (b) The corresponding distributions for $\psi(2S) \to l^+l^-$. (c) The combined $\psi(2S)\pi^+\pi^-$ invariant mass distribution for $\psi(2S) \to J/\psi\pi^+\pi^-$ and $\psi(2S) \to l^+l^-$. The solid curve shows the result of the fit. The dashed curve represents the background, while the dotted curves indicate the individual resonant contributions. Only one solution is found in this case.

background level in Fig. 1(a) is very low and that the results are not sensitive to the choice of the background parametrization function]. The parametrization of the signal function is described below. The fitted parameters are the masses, widths, and yields of the two resonances, the phase difference between the amplitudes of the two resonances, and the background yield and parameters. The result of the fit is shown by the solid curve in Fig. 1(a). We then perform an ML fit to the results of Fig. 1(c). The fitted parameters are the masses, the widths, the phase difference between the amplitudes of the two resonances, and the yields of the two resonances, which are treated independently for the $J/\psi\pi^+\pi^-$ and l^+l^- channels (four signal yields in total), and the yields and parameters of the background distributions for the two channels (two background yields in total). The background for the l^+l^- channel is treated by fitting a third-order polynomial to the distribution determined from the sideband while the background for the $J/\psi\pi^+\pi^-$ channel is treated as described above. The result of the fit is shown by the solid curve in Fig. 1(c).

The mass dependence of the signal function is given by $f(m) = \epsilon(m) \cdot \mathcal{L}(m) \cdot \sigma(m)$; $\epsilon(m)$ is the mass-dependent signal-selection efficiency obtained from a Monte Carlo (MC) simulation that uses a $\psi(2S)\pi^+\pi^-$ phase space distribution; its value increases from 1% at 3.95 GeV/c^2 to 12% at 5.95 GeV/c^2 for $\psi(2S) \to J/\psi\pi^+\pi^-$, and from 1% at 3.95 GeV/c^2 to 14% at 5.95 GeV/c^2 for $\psi(2S) \to l^+l^-$. The function $\mathcal{L}(m)$ is the mass-distributed luminosity [10] (we ignore the small corrections due to initial-state emission of additional soft photons); $\mathcal{L}(m)$ increases from 102 pb^{-1}/50 MeV to 202 pb^{-1}/50 MeV from 3.95 GeV/c^2 to 5.95 GeV/c^2.

The cross section, $\sigma(m)$, is described by the following function, which takes into account the possibility of interference between the two resonant amplitudes, since they have the same quantum numbers ($J^{PC} = 1^{--}$):

$$\sigma(m) = \frac{12\pi C}{m^2} \cdot |A_1(BW) \cdot \sqrt{\frac{PS(m)}{PS(m_1)}} + A_2(BW) \cdot \sqrt{\frac{PS(m)}{PS(m_2)}} \cdot e^{i\phi}|^2, \quad (1)$$

where $C = 0.3894 \times 10^9$ GeV^2 pb, and $PS(m)$ represents the mass dependence of $\psi(2S)\pi^+\pi^-$ phase space; ϕ is the relative phase between the amplitudes A_1 and A_2. The complex amplitude A_j is written as

$$A_j(BW) = \frac{m_j\sqrt{(\Gamma_{e^+e^-} \cdot \Gamma_{\psi(2S)\pi^+\pi^-})_j}}{m_j^2 - m^2 - im_j\Gamma_j}, \quad (2)$$

where m_j is the resonance mass and Γ_j its total width; $(\Gamma_{e^+e^-} \cdot \Gamma_{\psi(2S)\pi^+\pi^-})_j$ is the product of the partial widths to e^+e^- and to $\psi(2S)\pi^+\pi^-$.

In the fit procedure $f(m)$ is convolved with a Gaussian resolution function obtained from MC simulation. This function has a root-mean-squared deviation that increases linearly from 2 MeV/c^2 at $\sim$3.95 GeV/c^2 to 5 MeV/c^2 at $\sim$5.95 GeV/c^2. In the likelihood function, when the fit

TABLE I. Results of the fit to the $\psi(2S)\pi^+\pi^-$ invariant mass distributions for $\psi(2S) \to J/\psi\pi^+\pi^-$. The first errors are statistical and the second systematic; $\mathcal{B} \times \Gamma_{ee}$ is the product of the branching fraction to $\psi(2S)\pi^+\pi^-$ and the e^+e^- partial width (in eV), and ϕ is the relative phase between the two resonances (in degrees).

Parameters	First solution (constructive interference)	Second solution (destructive interference)
Mass $Y(4360)$ (MeV/c^2)	$4340 \pm 16 \pm 9$	
Width $Y(4360)$ (MeV)	$94 \pm 32 \pm 13$	
$\mathcal{B} \times \Gamma_{ee}(Y(4360))$ (eV)	$6.0 \pm 1.0 \pm 0.5$	$7.2 \pm 1.0 \pm 0.6$
Mass $Y(4660)$ (MeV/c^2)	$4669 \pm 21 \pm 3$	
Width $Y(4660)$ (MeV)	$104 \pm 48 \pm 10$	
$\mathcal{B} \times \Gamma_{ee}(Y(4660))$ (eV)	$2.7 \pm 1.3 \pm 0.5$	$7.5 \pm 1.7 \pm 0.7$
$\phi(^\circ)$	$12 \pm 27 \pm 4$	$-78 \pm 12 \pm 3$

is performed to the $\psi(2S) \to J/\psi\pi^+\pi^-$ data, $\sigma(m)$ is multiplied by $\mathcal{B}(\psi(2S) \to J/\psi\pi^+\pi^-) \times \mathcal{B}(J/\psi \to l^+l^-)$, since the fitted distribution corresponds to the observed event sample. Similarly, for $\psi(2S) \to l^+l^-$, $\sigma(m)$ is multiplied by $\mathcal{B}(\psi(2S) \to l^+l^-)$, where $l = e$ or μ.

The results of the fits are shown in Figs. 1(a) and 1(c), and the extracted parameters are summarized in Tables I and II, respectively. The significance of the $Y(4660)$ signal for both fits is 5.7σ where σ is the standard deviation.

For the fit to the distribution in Fig. 1(a), we obtain two solutions, one corresponding to constructive interference and one to destructive interference between the resonant amplitudes. The mass and the width values of the resonances are the same for each solution. However, the values of $\Gamma_{e^+e^-} \times \mathcal{B}(\psi(2S) \to J/\psi\pi^+\pi^-)$ and ϕ are different (see Table I), although the maximum likelihood value is exactly the same for each fit. The results summarized in Table I agree well with those obtained in the Belle analysis [6], for which the data sample is about the same size as that for the $\psi(2S) \to J/\psi\pi^+\pi^-$ decay mode in the present analysis [see Fig. 2(a)]. We infer that, even if our data sample for this mode were doubled in size, the ambiguity in the fit results would persist. For the fit to the distribution in Fig. 1(c), only one solution is found, corresponding to constructive interference. A second solution was expected, corresponding to destructive interference. However, a thorough examination of parameter space involving multiple, randomly chosen starting points yielded only one minimum in the likelihood function. The results of the fit, given in Table II, are consistent with the results of Table I. The inclusion of the $\psi(2S)$ dilepton data modes increases the number of signal events by around 40%, but at the expense of introducing a large background. Because of the large background, we discount the results summarized in Table II, and confine our attention to the results

TABLE II. Results of the fit to the combined $\psi(2S)\pi^+\pi^-$ invariant mass distributions for $\psi(2S) \to J/\psi\pi^+\pi^-$ and $\psi(2S) \to l^+l^-$. The uncertainties are statistical; $\mathcal{B} \times \Gamma_{ee}$ is the product of the branching fraction to $\psi(2S)\pi^+\pi^-$ and the e^+e^- partial width (in eV), and ϕ is the relative phase between the two resonances (in degrees).

Parameters	Solution
Mass $Y(4360)$ (MeV/c^2)	4318^{+15}_{-19}
Width $Y(4360)$ (MeV)	123 ± 20
$\mathcal{B} \times \Gamma_{ee}(Y(4360))$ (eV)	7.4 ± 0.9
Mass $Y(4660)$ (MeV/c^2)	4667^{+6}_{-7}
Width $Y(4660)$ (MeV)	36^{+32}_{-14}
$\mathcal{B} \times \Gamma_{ee}(Y(4660))$ (eV)	1.4 ± 0.5
$\phi(^\circ)$	25 ± 21

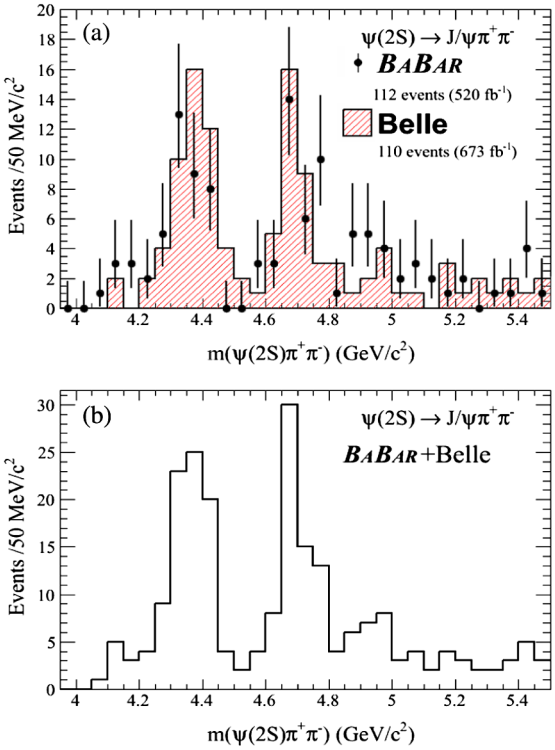

FIG. 2 (color online). (a) The comparison between the observed $\psi(2S)\pi^+\pi^-$ [$\psi(2S) \to J/\psi\pi^+\pi^-$] invariant mass spectrum from *BABAR* (dots) and that from Belle [6] (hatched histogram). (b) The combined *BABAR* and Belle $\psi(2S)\pi^+\pi^-$ [$\psi(2S) \to J/\psi\pi^+\pi^-$] invariant mass spectrum.

from $\psi(2S) \to J/\psi\pi^+\pi^-$ decay for the remainder of the analysis.

The fit results of Table I and the $\psi(2S)\pi^+\pi^-$ invariant mass spectrum of Fig 2(a) agree very well with those obtained by the Belle Collaboration [6]. Each distribution [Fig. 2(a)] shows evidence for two resonant structures (note that the Belle distribution ends at 5.5 GeV/c^2). This is even more apparent in Fig. 2(b), where we have added the distributions to obtain a mass spectrum corresponding to an integrated luminosity of ~ 1.2 ab^{-1}. The existence of two structures is quite clear, and there is even a hint of some activity in the vicinity of 5 GeV/c^2.

For the decay mode $\psi(2S) \to J/\psi\pi^+\pi^-$, we calculate the $e^+e^- \to \psi(2S)\pi^+\pi^-$ cross section after background subtraction for each $\psi(2S)\pi^+\pi^-$ mass interval, i, using

$$\sigma_i = \frac{n_i^{\rm obs} - n_i^{\rm bkg}}{\epsilon_i \cdot \mathcal{L}_i \cdot \mathcal{B}}, \tag{3}$$

where $n_i^{\rm obs}$ is the number of observed events, $n_i^{\rm bkg}$ is the number of background events, ϵ_i is the average efficiency, and $\mathcal{L}_i$ the integrated luminosity [10] for interval i; $\mathcal{B}$ represents the product $\mathcal{B}(\psi(2S) \to J/\psi\pi^+\pi^-) \cdot \mathcal{B}(J/\psi \to l^+l^-)$. The resulting dependence of the cross section on c.m. energy is shown in Fig. 3. We sum over the data points in Fig. 3 and obtain a model-independent integrated cross section value of 311^{+76}_{-30}(stat) $\pm$ 11(syst) pb for the region 3.95–5.95 GeV. The curve shown in Fig. 3 results from the fit to the data of Fig. 1(a) and provides an adequate description of the measured cross section.

Our estimates of systematic uncertainty result from the sources listed in Table III.

The systematic uncertainties on the fitted values of the $Y(4360)$ and the $Y(4660)$ parameters include contributions from the fitting procedure (evaluated by changing the fit range and the background parametrization), the uncertainty in the mass scale (which results from the uncertainties associated with the magnetic field and with our energy-loss correction procedures [11,12]), the mass-resolution function, and the change in efficiency when the dipion distribution is simulated using the histograms in Fig. 4. Uncertainties associated with luminosity, tracking, efficiency, and PID affect only $\Gamma_{e^+e^-} \cdot \mathcal{B}$, and their net contribution is 3.3%. Uncertainties on the relevant branching fraction values [9] are indicated in Table III and are relevant only for $\Gamma_{e^+e^-} \cdot \mathcal{B}$. These estimates of systematic uncertainty are combined in quadrature to obtain the values which we quote for the $Y(4360)$ and $Y(4660)$ states.

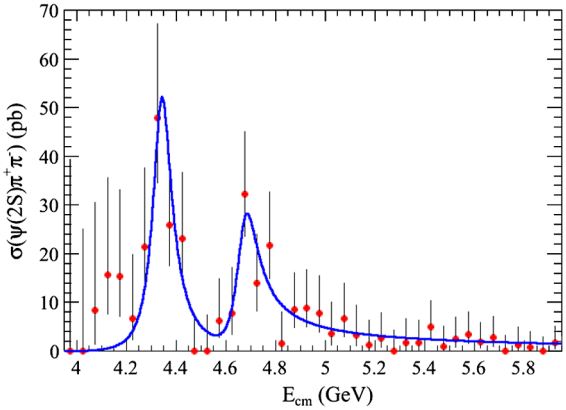

FIG. 3 (color online). The cross section for the reaction $e^+e^- \to \psi(2S)\pi^+\pi^-$ as a function of c.m. energy obtained by using Eq. (3) (points with error bars); the curve shows the c.m. energy dependence which results from the fit to the data of Fig. 1(a).

In Fig. 4 we show the $\pi^+\pi^-$ invariant mass distributions for events in the $\psi(2S)\pi^+\pi^-$, $\psi(2S) \to J/\psi\pi^+\pi^-$ invariant mass regions (a) 4.0 GeV/c^2 $< m_{\psi(2S)\pi^+\pi^-} <$ 4.5 GeV/c^2, and (b) 4.5 GeV/c^2 $< m_{\psi(2S)\pi^+\pi^-} <$ 4.9 GeV/c^2. The distributions are consistent with previous measurements [6]. In each case, the mass distribution appears to differ slightly from the phase-space expectation, as shown by the corresponding histogram. For the higher mass

TABLE III. Systematic uncertainty estimates for the parameters used in the fit to the data of Fig. 1(a).

Source	$\Gamma_{e^+e^-} \cdot \mathcal{B}$ (%) (constructive interference)	$\Gamma_{e^+e^-} \cdot \mathcal{B}$ (%) (destructive interference)	Mass (MeV/c^2)	Γ (MeV)
Fit procedure for the $Y(4360)$	$\pm$2.5	$\pm$1.4	$\pm$9	$\pm$13
Fit procedure for the $Y(4660)$	$\pm$14	$\pm$3.3	$\pm$3	$\pm$10
Mass scale	⋯	⋯	$\pm$0.5	⋯
Mass resolution	⋯	⋯	⋯	$\pm$1.3
MC dipion model	$\pm$6.8	$\pm$6.8	⋯	⋯
$\mathcal{B}_{(\psi(2S)\to J/\psi\pi^+\pi^-)}$	$\pm$1.2	$\pm$1.2	⋯	⋯
$\mathcal{B}_{(J/\psi\to l^+l^-)}$	$\pm$0.7	$\pm$0.7	⋯	⋯
PID, luminosity and tracking	$\pm$3.3	$\pm$3.3	⋯	⋯
Total ($Y(4360)$)	$\pm$8	$\pm$8	$\pm$9	$\pm$13
Total ($Y(4660)$)	$\pm$16	$\pm$6	$\pm$3	$\pm$10

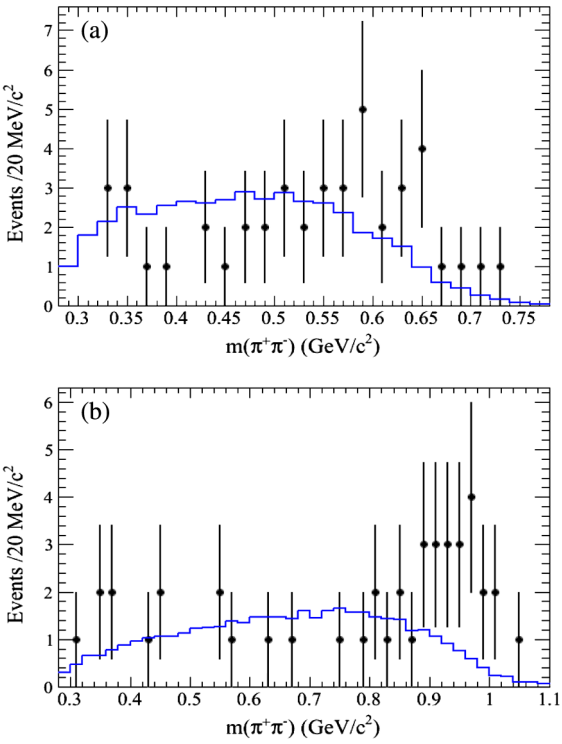

FIG. 4 (color online). The $\pi^+\pi^-$ invariant mass spectrum for the $\psi(2S) \to J/\psi\pi^+\pi^-$ channel in the $\psi(2S)\pi^+\pi^-$ mass region (a) 4.0–4.5 GeV/c^2, and (b) 4.5–4.9 GeV/c^2. The histogram represents a MC distribution corresponding to the decay according to phase space of (a) one resonance with a mass of 4.360 GeV/c^2 and width 70 MeV, and (b) one resonance with a mass of 4.660 GeV/c^2 and width 50 MeV. Each histogram is normalized to the corresponding data sample.

resonance, there is some indication of an accumulation of events in the vicinity of the $f_0(980)$ state. Similar behavior is observed in [6], and both distributions bear a qualitative resemblance to the dipion invariant mass spectrum from the decay $Y(4260) \to J/\psi\pi^+\pi^-$ [13]. The small number of events involved precludes the drawing of any definite conclusion.

In summary, we have used ISR events to study the reaction $e^+e^- \to \psi(2S)\pi^+\pi^-$ in the c.m. energy range 3.95–5.95 GeV. We observe two resonant structures, which we interpret as the $Y(4360)$ and the $Y(4660)$, respectively. For the $Y(4360)$ we obtain $m = 4340 \pm 16 \pm 9$ MeV/c^2 and $\Gamma = 94 \pm 32 \pm 13$ MeV, and for the $Y(4660)$ $m = 4669 \pm 21 \pm 3$ MeV/c^2 and $\Gamma = 104 \pm 48 \pm 10$ MeV; in each case the first uncertainty is statistical and the second is systematic. We thus confirm the report in Ref. [6] of a structure near 4.65 GeV/c^2 and obtain consistent parameter values for this state. If we include the $Y(4260)$, which decays to $J/\psi\pi^+\pi^-$ [4], three charmoniumlike states with $J^{PC} = 1^{--}$ have been observed in the mass region 4.2–4.7 GeV/c^2, none of which has a well-understood interpretation.

ACKNOWLEDGMENTS

We are grateful for the excellent luminosity and machine conditions provided by our PEP-II2 colleagues, and for the substantial dedicated effort from the computing organizations that support *BABAR*. The collaborating institutions wish to thank SLAC for its support and kind hospitality. This work is supported by DOE and NSF (USA), NSERC (Canada), CEA and CNRS-IN2P3 (France), BMBF and DFG (Germany), INFN (Italy), FOM (The Netherlands), NFR (Norway), MES (Russia), MICIIN (Spain), and STFC (United Kingdom). Individuals have received support from the Marie Curie EIF (European Union) and the A. P. Sloan Foundation (U.S.A).

[1] S. K. Choi *et al.* (Belle Collaboration), Phys. Rev. Lett. **91**, 262001 (2003).
[2] S. Uehara *et al.* (Belle Collaboration), Phys. Rev. Lett. **96**, 082003 (2006).
[3] S. K. Choi *et al.* (Belle Collaboration), Phys. Rev. Lett. **94**, 182002 (2005).
[4] B. Aubert *et al.* (*BABAR* Collaboration), Phys. Rev. Lett. **95**, 142001 (2005).
[5] B. Aubert *et al.* (*BABAR* Collaboration), Phys. Rev. Lett. **98**, 212001 (2007).
[6] X. L. Wang *et al.* (Belle Collaboration), Phys. Rev. Lett. **99**, 142002 (2007).
[7] J. P. Lees *et al.* (*BABAR* Collaboration), Nucl. Instrum. Methods Phys. Res., Sect. A **726**, 203 (2013).
[8] B. Aubert *et al.* (*BABAR* Collaboration), Nucl. Instrum. Methods Phys. Res., Sect. A **479**, 1 (2002); , Nucl. Instrum. Methods Phys. Res., Sect. A **729**, 615 (2013).
[9] K. Nakamura *et al.* (Particle Data Group), J. Phys. G **37**, 075021 (2010), and partial update for the 2012 edition (URL: http://pdg.lbl.gov).
[10] E. A. Kuraev and V. S. Fadin, Sov. J. Nucl. Phys. **41**, 466 (1985).
[11] B. Aubert *et al.* (*BABAR* Collaboration), Phys. Rev. D **72**, 052006 (2005).
[12] B. Aubert *et al.* (*BABAR* Collaboration), Phys. Rev. D **80**, 092005(R) (2009).
[13] J. P. Lees *et al.* (*BABAR* Collaboration), Phys. Rev. D **86**, 051102(R) (2012).